Simulation and Design of the Geometric Characteristics of the Oscillatory Thermal Cycler

Tse-Yu Hsieh, and Jyh-Jian Chen

Abstract—Since polymerase chain reaction (PCR) has been invented, it has emerged as a powerful tool in genetic analysis. The PCR products are closely linked with thermal cycles. Therefore, to reduce the reaction time and make temperature distribution uniform in the reaction chamber, a novel oscillatory thermal cycler is designed. The sample is placed in a fixed chamber, and three constant isothermal zones are established and lined in the system. The sample is oscillated and contacted with three different isothermal zones to complete thermal cycles. This study presents the design of the geometric characteristics of the chamber. The commercial software CFD-ACE^{+TM} is utilized to investigate the influences of various materials, heating times, chamber volumes, and moving speed of the chamber on the temperature distributions inside the chamber. The chamber moves at a specific velocity and the boundary conditions with time variations are related to the moving speed. Whereas the chamber moves, the boundary is specified at the conditions of the convection or the uniform temperature. The user subroutines compiled by the FORTRAN language are used to make the numerical results realistically. Results show that the reaction chamber with a rectangular prism is heated on six faces; the effects of various moving speeds of the chamber on the temperature distributions are examined. Regarding to the temperature profiles and the standard deviation of the temperature at the Y-cut cross section, the non-uniform temperature inside chamber is found as the moving speed is larger than 0.01 m/s. By reducing the heating faces to four, the standard deviation of the temperature of the reaction chamber is under 1.4×10^{-3}K with the range of velocities between 0.0001 m/s and 1 m/s. The nature convective boundary conditions are set at all boundaries while the chamber moves between two heaters, the effects of various moving velocities of the chamber on the temperature distributions are negligible at the assigned time duration.

Keywords—Polymerase chain reaction, oscillatory thermal cycler, standard deviation of temperature, nature convective.

I. INTRODUCTION

SINCE polymerase chain reaction (PCR) has been invented in the early 1980s by Mullis et al. [1], for which he was awarded the Nobel Prize for Chemistry in 1993, PCR has developed into the standard method for the identification and replication of DNA strands. The PCR process consists of three steps. (1) Denaturation: double-stranded DNA is separated into two single strands at high temperature (95°C), (2) Annealing: primers bind their complementary site of the single-stranded DNAs at low temperature (55°C), and (3) Extension: these DNA strands are extended by thermos table DNA polymerase enzyme at intermediate temperature (72°C) [2]. Nowadays the PCR process mostly is carried on in the thermal cycler. The PCR amplification efficiency is not only related to the sample pre-preparation, but also the temperature distribution of the sample as the sample moves through the thermal cycler. In order to complete the PCR process accurately, a precise heat transfer mechanism is necessary.

The manipulation methods of the PCR chip can be categorized into the chamber type and the continuous flow type. The chamber type devices are a microfabricated version of conventional thermal cyclers. The mixture is kept stationary, and the temperature of the reaction chamber is cycled. In 1993, Nothrup et al. [3] presented the first microfabicated PCR chip. They fabricated PCR reaction chambers in silicon with various volumes up to 50 μl. The chambers were formed by bonding two processed silicon wafers with polyimide. The chamber type chip contains a reaction chamber with an integrated heating system that changes in temperature with time. However, these devices are highly integrated featuring different metals for rapid heating, active cooling and temperature control, so a rather complex and expensive fabrication procedure is required. For the continuous flow type (CFPCR Chip), the reaction mixture moves through three different isothermal zones in a thin channel instead of cycling the temperature of whole device. In 1998, Kopp et al. [4] presented the first CFPCR chip. The chip was fabricated in the Corning 0211 glass and all channels were 40 μm deep and 90 μm wide. The etched glass chip and the cover plate were each 0.55 mm thick. The chip was put on three copper blocks which were heated by 5 W heating cartridges and set at three process temperatures.

In 2002, Zhang et al. [5] used finite element analysis (FEA) to investigate the temperature patterns of continuous flow micro PCR chips: glass/glass bonding chip and silicon/glass bonding chip. Between these two thin chips, the values of the temperature gradient are approximately the same. Moreover there are three individual isothermal zones created in the

T. Y. Hsieh is with National Pingtung University of Science and Technology, 1, Hseuh Fu Road, Nei Pu, Pingtung 912, Taiwan, ROC (e-mail: m9644007@ mail.npust.edu.tw).

J. J. Chen is with National Pingtung University of Science and Technology, 1, Hseuh Fu Road, Nei Pu, Pingtung 912, Taiwan, ROC (corresponding author to provide phone: 886-87703202-7029; fax: 886-87740420; e-mail: chaucer@ mail.npust.edu.tw).

World Academy of Science, Engineering and Technology
International Journal of Materials and Metallurgical Engineering
Vol:3, No:5, 2009

CFPCR chip through which the mixture passes. So, in order to achieve thermal isolation of the individual reaction zones and prevent the cross talking, the arrangement of the heaters is very important. In 2002, Chou et al. [6] used CFD-ACE^{+TM} to simulate the temperature distribution inside the chip and then fabricated the first miniaturized cyclic PCR device. There existed two air gaps in the device to make three isothermal zones separately and avoid cross talking. This PCR device with the flow rate of 15 μl/min drive the buffer to complete 30 cycles within less than 40 min. In 2003, Bu et al. [7] designed a novel CFPCR chip with an integrated micro peristaltic pump and three chambers. The sample moved back and forth between the chambers by the micro pump for sample reaction. After utilizing the finite element simulation (FEM) for the optimization of the geometry of the reaction chamber and the location of heater, results were found that the sample could be heated/cooled in the proposed device in less than 1 s to achieve the desired temperatures. Inside the CFPCR Chip, the sample had a high heating and cooling velocity which was dependent of the flow speed. In 2004, Hashimoto et al. [8] developed a CFPCR device which could reduce the amplification time by increasing the flow velocity through the isothermal zones. They also used FEA to investigate the heat transfer mechanism along a single channel and the effects of various channel radii on the temperature distribution in the CFPCR device. In 2008, Joung et al. [9] proposed a CFPCR chip which used the indium-tin-oxide (ITO) coated glass as the thin film heaters, and polydimethylsiloxane (PDMS) as the microchannel. They investigated the influences of various flow rates on the DNA amplification. The result showed that at low flow rates, the amplification of the PCR product was not guaranteed. Besides, the system with a faster flow rate generated less PCR product. The optimum flow rate of this particular CFPCR chip was 4 μl/min and the total reaction time was 14 min for 20 cycles. The flow rate inside the channel is related to the arrangement and characteristics of the channel. So the arrangement of the channel network is necessary for the design of the PCR system. In 2005, Xiaoyu et al. [10] developed a novel CFPCR chip with a spiral channel made by PDMS and glass. The channel was placed around the heaters. They also used FEA software ANSYS and FLUENT to optimize the design of the chip and performed the temperature distribution of three isothermal zones and the velocity profiles within various cross-section areas along the microchannel. After the evaluation of the CFPCR chip, results showed the chip with spiral channel arrangement could improve the productivity and efficiency effectively. In 2007, Tsai et al. [11] designed a continuous flow μRT-PCR chip. The most important issue in the chip was the creation of the precise temperature distribution of the four heated zones and the flow rate in the channel. They used commercial software ANSYS, CFD-ACE+TM, and IntelliSuite to simulate the temperature distribution in the isothermal zone and the effective fluid flow, especially at the turning corners of the microchannels. They obtained the optimal flow rate to avoid the clogging problem. Even if CFPCR has many merits such as no needing the cooling system, there are still many obstacles to be overcome in the high temperature sensitivity reactions, such as that the temperature uniformity is not good, the thermal process cannot be adjusted and the air bubbles are generated in the microchannels. In 2006, Nakayama et al. [12] found the air bubbles were generated in the microchannels, which might decrease the solubility of gas in the sample and hinder the sample to move through the microchannels. They avoided the generation of air bubbles by adding highly viscous liquid into the fluid.

The PCR chip has the problems such as the price is too expensive and the fabrication is too complex. Also, the PCR product still needs to carry on the detection in the laboratory. Therefore the PCR chip has been unavailable for most people. Currently many PCR chips are integrated the ancillary equipments such as thermal cycler, pump, and fluorescence detection to perform the real-time detection. In 2007, Gärtner et al. [13] presented a system comprising a SU-8 CFPCR chip and a thermal cycler unit. The thermal cycler unit could heat two PCR chips simultaneously, so it improved the DNA amplification efficiency. In 2008, Crews et al. [14] designed the first CFPCR device within a single steady state isothermal zone. They put the chip on two aluminum stripes. The thin-film heaters were fixed beneath one stripe. The other stripe corresponding to the cooler edge was coupled to a network of cooling fins. A thermal gradient was induced across the glass by heating one stripe. By changing the width of the channels, it could adjust the velocity of the sample in the channel. This thermal gradient technique was capable of rapid DNA amplification, which could complete 40 cycles in just 9 min. In 2008, Lee et al. [15] developed a novel real-time PCR machine containing a temperature sensor array to monitor the thermal cycling profiles of PCR system. A fluorescence detection system consisted of a cooled CCD in order to determine the DNA amplification efficiencies of each cycle in real-time detection. Compared with the CFPCR chip, the conventional PCR machine is composed of the fixed heating blocks, where the heating and the cooling rate is approximately 4°C-5°C/s (slower than the PCR chip), and the temperature distribution in the system is also non-uniform. However, the cost of the PCR machine is low, and PCR system can be easily integrated with the ancillary equipments. If the volume can be reduced, the PCR machine will probably be more suitable than the PCR chip in practice applications. So we designed an OScillatory TheRmal cYcler CHamber (OSTRYCH) which combined with the merits of the chamber-type PCR Chip and the CFPCR Chip. The samples are placed in a fixed chamber. Three isothermal zones are established in the system. The samples are oscillated and contacted with three different isothermal zones to complete the thermal cyclers.

This study presents the effects of the geometric characteristics on the temperature of the PCR chamber. The commercial software CFD-ACE^{+TM} is used to investigate the temperature distributions in the chamber by a 3-D transient model. The chamber moves at a specific velocity, and the boundary conditions with time variation are related with the

World Academy of Science, Engineering and Technology
International Journal of Materials and Metallurgical Engineering
Vol:3, No:5, 2009

moving speed. The user subroutines compiled by the FORTRAN language are utilized to assure the numerical results realistically. Using air convection coefficient and/or isothermal heating, the effects of various boundary conditions on the temperature distribution in the chamber during the chamber passing through three isothermal zones with different velocities are discussed.

II. THEORETICAL MODEL

In this study, the chamber oscillates among three isothermal zones. The chamber absorbs the thermal energy and then the thermal energy is transmitted to the buffer. As the PCR chamber passes between two isothermal zones, the heat will be transferred by the ambient air. The heat transfer mechanisms contain thermal conduction and heat convection.
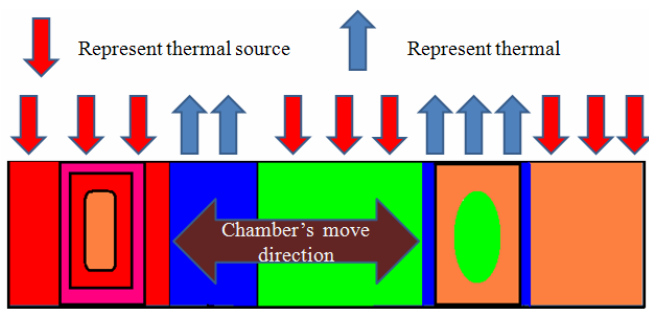

Fig. 1 Schematic diagram of the PCR system

The energy is transferred from the region with high temperature to that with low temperature. At the steady state, one-dimensional heat conduction can be expressed with the Fourier's Law

$$q = -kA_{cond} \frac{\Delta T}{\Delta x} \tag{1}$$

where k is the thermal conductivity, which is the property of a material that indicates its ability to conduct heat. Heat convection is the mechanism that the heat is transferred by the movement of a fluid, and the heat convection coefficient responses to the thermal transfer efficiency. It can be expressed with the Newton's law of cooling

$$q = h_c A_{conv} \Delta T \tag{2}$$

Substances with high thermal diffusivity rapidly adjust their temperature to that of their surroundings, because they conduct heat quickly comparison with the storage of energy in their volumetric elements. The thermal diffusivity can be expressed as

$$\alpha = \frac{k}{\rho c} \tag{3}$$

where α is the thermal diffusivity, c is the specific heat capacity,

and ρ is the density. In addition, the boundary conditions, the moving velocity and the thermal properties of the materials are all related to the chamber temperature whereas the chamber is moving in the system. In this work, the chamber moves through different isothermal zones. The boundary conditions are changed with time, and related to the moving velocity. The governing equations can be expressed as

$$\rho c \frac{\partial T}{\partial \tau} + \rho c U \frac{\partial T}{\partial x} + \rho c V \frac{\partial T}{\partial y} + \rho c W \frac{\partial T}{\partial z}$$
$$= k \frac{\partial^2 T}{\partial x^2} + k \frac{\partial^2 T}{\partial y^2} + k \frac{\partial^2 T}{\partial z^2} \tag{4}$$

where τ is time. The FEA method is used to solve the energy field and to obtain the transient temperature.

III. NUMERICAL METHODS

A simulation software CFD-ACE^{+TM} to examine the three-dimensional temperature distribution of the reaction chamber is used, and the numerical method is the finite volume method. The solution domain is divided into a number of cells known as control volumes. In the finite volume approach of CFD-ACE^{+TM}, the governing equations are numerically integrated over each of these computational cells or control volumes. The geometric center of the control volume is also often referred to as the cell center. CFD-ACE^{+TM} employs a co-located cell-centered variable arrangement, all dependent variables and material properties are stored at the cell center. In other words, the average value of any quantity within a control volume is given by its value at the cell center. Most of the governing equations can be expressed in the form of a generalized transport equation

$$\frac{\partial \rho \phi}{\partial \tau} + \nabla \bullet \left(\rho \vec{V} \phi \right) = \nabla \bullet \left(\Gamma \nabla \phi \right) + S_\phi \tag{5}$$

Each term of the generalized equation from left to right is transient, convection, diffusion and source term, respectively. φ represents the user defined quantity in the generic conservation equation, such as enthalpy.

The grid generation section can be divided into the structured grid and the unstructured grid. The structured grid with good orthogonality is recommended for accurate prediction and reliability. However, the unstructured grids have the geometric flexibility and can be adapted according to flow features. The structured grids build the 3-D structure which can be composed of hexahedron. In this study the geometric model for the three dimensional rectangular structure is considered. Therefore, the structured grid system is utilized directly.

CFD-ACE^{+TM} calculating heat transfer module utilizes the conservation equation for energy as the governing equation. The all enthalpy equation which infers energy equation is as

World Academy of Science, Engineering and Technology
International Journal of Materials and Metallurgical Engineering
Vol:3, No:5, 2009

follows

$$\frac{\partial \rho h_0}{\partial \tau} + \nabla \bullet \left(\rho \vec{V} h_0 \right) = \nabla \bullet \left(k \nabla h_0 \right) + \frac{\partial p}{\partial \tau} \qquad (6)$$

h_0 can be expressed as

$$h_0 = i + \frac{p}{\rho} + \frac{1}{2} \left(u^2 + v^2 + w^2 \right) \qquad (7)$$

where h0 is the enthalpy, i is the internal energy, and p is static pressure, u, v, and w are the moving speed of the molecules at x, y and z directions. In this case, it does not need to consider the static pressure and the moving speed of the solid molecules. In the computation of the enthalpy of the simulation model, the first-order upwind scheme is chosen because it has the first-order accuracy and is one of the most stable schemes. In the convergence part, because each physical quantity in each control volume during each iteration does not necessarily satisfy the conservation equation, solving the residual value is the important indication to judge the convergence. The residual value can be expressed as

$$R = \left| \left(Q_C^{n+1} - Q_C^n \right) + \left(Q_d^{n+1} - Q_d^n \right) + \left(Q_S^{n+1} - Q_S^n \right) \right| dV_{cell} \qquad (8)$$

where Q_C is the convection term, Qd is the diffusion term, Q_S is the source term, and dVcell is the volume of cell. In this case, the CGS+Pre (conjugate gradient squared plus preconditioning) solver in CFD-ACE[+TM] is chosen. The conditions of convergence can be divided into two kinds. The first one is the maximum number of the solver iterations. The second one determines the convergence criteria to be used. In this study, we perform 500 sweep times and use 10^{-4} as the convergence criterion.

The relaxation coefficient for each solved variables and for the auxiliary variables can be adjusted. Under relaxation is a constraint on the change of a dependent or auxiliary variable from one solution iteration to the next. It is not only required to maintain the stability of the coupled, non-linear system of equations, but also used to constrain the change in the variable from iteration to iteration in order to prevent divergence of the solution procedure. CFD-ACE[+TM] uses linear relaxation and inertial relaxation to improve the convergence speed. The linear relaxation value is from 0 to 1. A larger linear relaxation indicates that the initial value is close to the newest convergence value. A smaller value indicates the value is close to the last convergence value. For the inertial relaxation, a smaller value indicates that the initial value is close to the newest convergence value, and a larger value indicates the value is close to the last convergence value. The relaxation coefficient is remained at the default values.

IV. RESULTS AND DISCUSSION

Before simulating the temperature distributions of the chamber moving through three isothermal zones, the influences of various material properties on the heat transfer are investigated. Stainless steel, aluminum, copper, and iron are selected to do the simulations. Table I lists the thermal parameters of the four materials. In order to examine the effects of the material properties on heat transfer, a volume of a cubic is set, and six heating faces with temperature of 390K are assigned. The heating time is 6 s, and the initial temperature is equal to 300K. As shown in Fig. 2, the results show that the volume center temperature of copper achieves 390K in 1.2 s; that of aluminum achieves 390K in 1.4 s; that of iron achieves 390K in 3.7 s; and that of stainless steel achieves 390K in 5.7 s. Compared with the thermal diffusivity presented in Table I, the metal which has the largest thermal diffusivity can achieve the temperature of 390K in the shortest time. The required times that the volumes made of aluminum and copper achieve the target temperature are almost the same. Regarding to the system weight and the cost, aluminum is chosen as the material of the PCR chamber.

TABLE I
THE THERMAL PARAMETERS OF THE FOUR MATERIALS

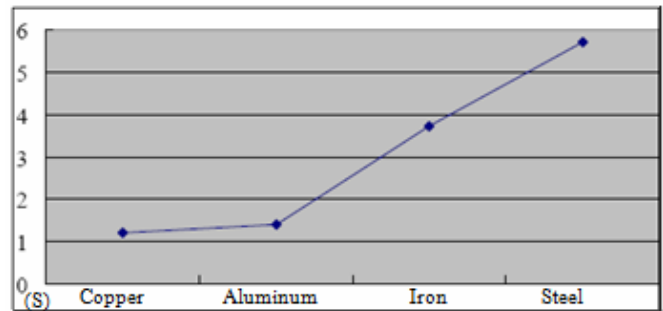| Material	Density (kg/m³)	Thermal conductivity (W/m-K)	Specific heat capacity (J/Kg-K)	Thermal diffusivity (m²/s)
Stainless Steel	7900.0	348	490	1.2390×10^{-5}
Aluminum	2698.9	210	900	8.6454×10^{-5}
Copper	8960.0	385	385	11.1607×10^{-5}
Iron	7870.0	76.2	440	2.2005×10^{-5}

Fig. 2 The required time to achieve the temperature of 390K for the volumes made of four materials

The length, width and height of the chamber are 0.8 cm, 0.6 cm, and 0.6 cm, respectively, and the chamber wall thickness is 0.1 cm, so the reaction chamber can contain a buffer volume of 96 μl. The commercial PCR system needs a buffer volume of approximately 25 μl. It's no doubt that a smaller volume of 25-μl reactants can be performed the PCR in the present system whereas the PCR process can be completed with a buffer volume of 96 μl. In this case, six isothermal faces are set at the boundaries of chamber, and the chamber moves through three isothermal zones at the temperature of 368K, 318K, and 345K in 300s. Between two isothermal zones the boundary conditions of the chamber are all set at 300K. The variations of

World Academy of Science, Engineering and Technology
International Journal of Materials and Metallurgical Engineering
Vol:3, No:5, 2009

the boundary conditions of the chamber along with time is shown in Fig. 3(a), and "+" expresses the temperature at the time of 0, 30, 60, 90, 120, 150, 180, 210, 270, and 300 seconds, respectively. The reaction times during the three isothermal zones are 30-60s, 120-150s, and 210-270s, respectively. The simulation reaction times are the same as the reaction times which are the needed reaction times at the commercial PCR system. The ratio of the heating time is 1:1:2 and the reaction time of extension double that of annealing and denaturation. The thermal boundary condition is isothermal, and the influences of various moving speed of the chamber on temperature are examined. The moving speed is 0.0001 m/s, 0.0005 m/s, 0.001 m/s, 0.005 m/s, 0.01 m/s, 0.05 m/s, 0.1 m/s, 0.5 m/s and 1 m/s, respectively. Simulation results of the central temperature of the chamber are shown in Fig. 3(b). The result shows that the center temperature of the chamber can achieve the reaction temperature during the reaction time and the temperatures are almost the same as the moving speed is less than 0.1 m/s. However the moving speed is beyond the value of 0.1 m/s, the center temperature of the chamber is higher than the required reaction temperature before entering the isothermal zone. After entering the isothermal zones the thermal energy cannot be transferred into the ambient region and the temperature of chamber starts to increase. The standard deviations of the temperature at Y-cut cross section at various moving speed at the time of 150 s are shown in Fig. 3(c). This cross section is the X-Z surface plane of symmetry of the chamber, and there is a symmetric axis at Z-direction at the chamber. Therefore the results shown in Fig. 3(c) can be extended to the whole volume. From the simulated results, the standard deviation is less than 1K as the traveling speed under 0.01 m/s. It means that the variations of the temperature distribution at the cross section are less than 1K. It also expresses that the variations of the temperature distribution of the chamber are less than 1K. This result satisfies the requested temperature precision of the commercial PCR.
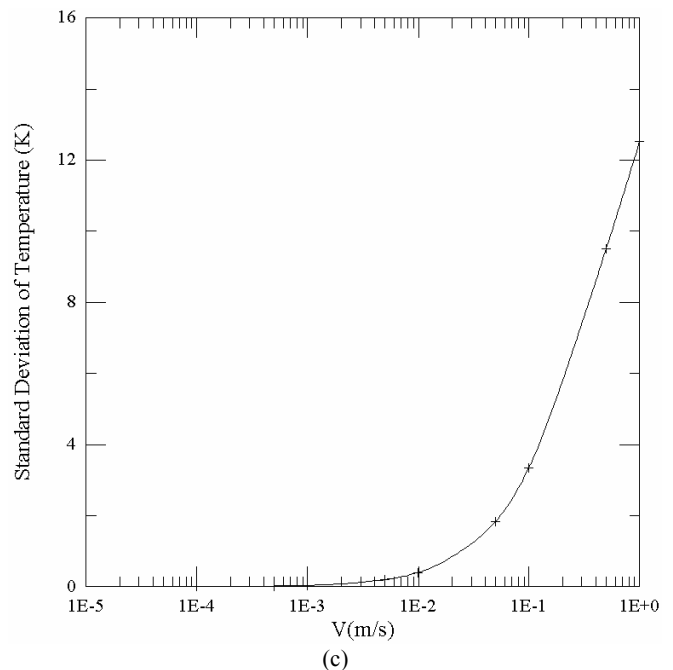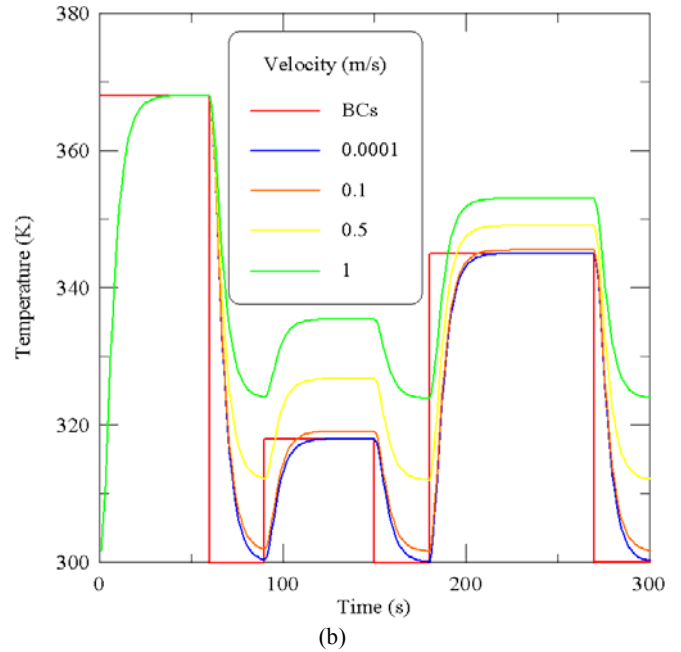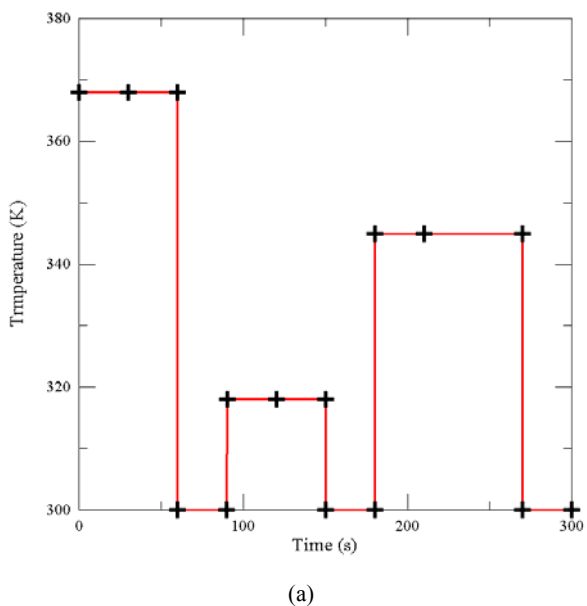

(b)

(c)

Fig. 3 (a) The variations of the boundary conditions of the chamber with time (b) the center temperature profiles of chamber (c) the standard deviation profiles of the temperature at a specific cross section

The influences of various moving speeds of the chamber on the cross-sectional temperature distributions at time of 60 s, 150 s, and 270 s are shown in Fig. 4 and Fig. 5. The moving speed is 0.01 m/s and 1 m/s, respectively. Fig. (a), (b) and (c) show the temperature profiles whereas the chamber passes through the three isothermal zones and completes each reaction. It's found that as the moving speed is 0.01 m/s, and the temperature is higher at the back side of the chamber than the other region shown in Fig. 4. This means that the temperature

(a)

World Academy of Science, Engineering and Technology
International Journal of Materials and Metallurgical Engineering
Vol:3, No:5, 2009

distribution is non-uniform inside the chamber. As the moving speed is increased to 1 m/s, the non-uniformity of the temperature distribution is much more obvious shown in Fig. 5. It's because that the chamber enters the isothermal zone of 368K, the internal temperature of the buffer is increased to 368K. After passing through the isothermal zone and the non-heating zone the chamber enters another isothermal zone. The moving speed is fast and the time duration during the non-heating zone is short, and only a little thermal energy of the chamber can be transferred to the ambient region by the air convection. The temperature of the chamber is not decreased before entering the next isothermal zone. The isothermal boundary conditions are set at six faces, and the thermal energy on the back side of the chamber is unable to reduce. Then the non-uniformity effect of the temperature can be observed at the back side of the chamber.
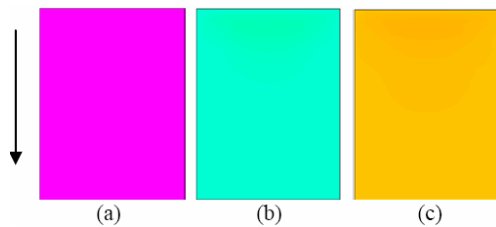

Fig. 4 At the moving speed of 0.01 m/s, the temperature distribution of Y-half cut cross section at (a) 60 s, (b) 150 s, (c) 270 s.
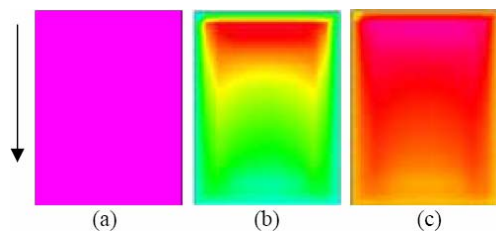

Fig. 5 At the moving speed of 1 m/s, the temperature distribution of Y-half cut cross section at (a) 60 s, (b) 150 s, (c) 270 s.

In order to improve the temperature uniformity, the number of the heating faces is reduced from six to four as shown in Fig. 6. The heat of the back and front side faces of the chamber are transferred by convection. The heat transfer coefficient is set to be 10 W/m^2K, and the ambient temperature is 300K. Simulation results of the center temperature profiles of the chamber at various moving speeds are revealed in Fig. 7(a). From the results, the faster moving speed is, the more uniform result of the temperature distribution appears. The central temperature of the chamber at the moving speeds from 0.0001 m/s to 1 m/s can achieve the target temperature. In addition the standard deviations of the temperature at Y-half cut cross section are compared as shown in Fig. 7(b). The time is 150 s after the reaction starting, and the chamber moves at the speed from 0.0001 m/s to 1 m/s. The results demonstrate that the standard deviations of the temperature distributions are all within 1.2×10^{-3}K, and it also means that the standard deviations of the temperature distributions in the chamber are within 1.2×10^{-3}K. The result shows a better uniformity of the

temperature of four heating boundaries than that of six boundaries.
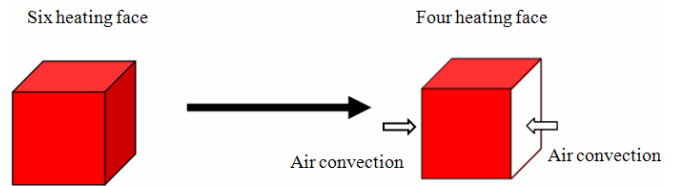

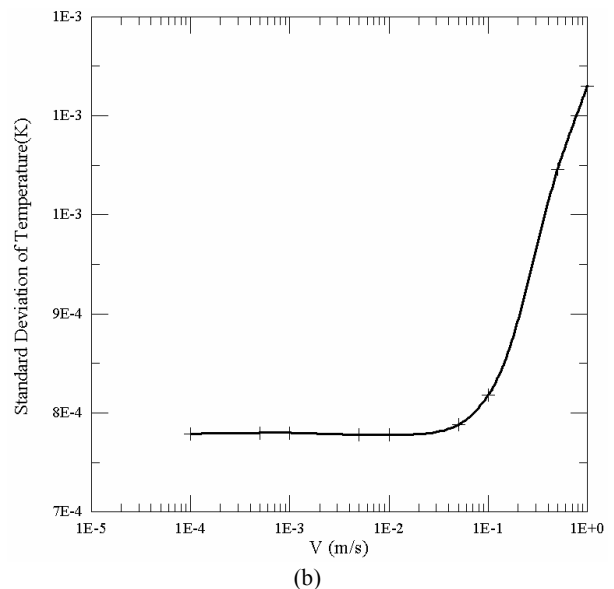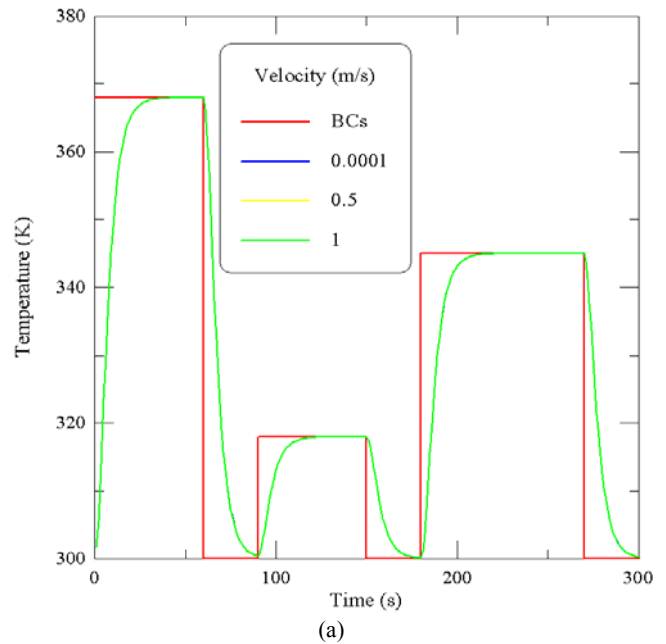Fig. 6 The schematic diagram of the boundary conditions changed

Fig. 7 (a) the center temperature profiles of chamber (b) the standard deviation profiles of the temperature at a specific cross section

In order to examine the reason of the reduction of the temperature standard deviation, the temperature distributions of Y-half cut cross section at three different times of 60 s, 150 s,

World Academy of Science, Engineering and Technology
International Journal of Materials and Metallurgical Engineering
Vol:3, No:5, 2009

and 270 s are illustrated in Fig. 8, respectively. The chamber moves at the speed of 1 m/s. From Fig. 8 the heating faces of the chamber are reduced to four, and the temperature non-uniformity at the back side of the chamber is disappeared. At the time of 150 s, the temperature standard deviation of the chamber also becomes less than 1.2×10^{-3}K. This is because the conditions of the back and front sides are changed from isothermal heating to air convection, the thermal energy can be carried away by the air. So the non-uniformity of the temperature distribution inside chamber is not appeared.
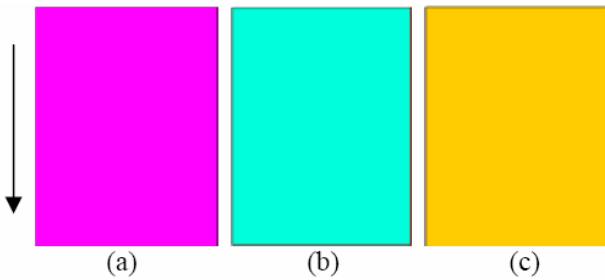

Fig. 8 At the moving speed of 1 m/s, the temperature distribution of Y-half cut cross section at (a) 60 s, (b) 150 s, (c) 270 s

The isothermal boundary conditions are chosen since the chamber moving through three isothermal zones has a very good contact with the heating blocks. However, the chamber moves between the isothermal regions, and the isothermal boundary condition of 300K is not realistic. To simulate the realistic boundary condition of the chamber, the air convection condition should be the boundary condition. Utilizing the CFD-ACE^{+TM}, the user subroutines compiled by FORTRAN language are used to set the isothermal boundary conditions of four faces of the chamber during the three isothermal zones (368K, 318K, and 345K) and the air convective boundary conditions between the isothermal regions. In order to simplify the subroutines, the heat convection coefficient is taken as infinitely to approximately simulate the isothermal heating process. However, the assigned boundary condition of infinite heat convection coefficient cost a lot of computational time during numerical simulation. A proper value of heat convection coefficient which does not affect the accuracy of the simulation results and not spend too much computational time should be found. A 2-D square model is used to find the proper value of heat convective coefficient as shown in Fig. 9(a). The boundary conditions of the left and bottom sides are set with air convection, and the air convection coefficient is 10 W/m²K. The ambient temperature is 380K. The boundary condition of the top side is heat convection with the convection coefficient of 10 W/m²K and the ambient temperature of 320 K. The boundary condition of the right side is set at the isothermal condition of 320K. In numerical simulation, the air convection coefficient of the right side, hc, is set in the user subroutine from 200 to 10^6 W/m²K. The computed results of the center temperature of the square can be expressed in Fig. 9(b). The result shows that hc is between the values of 2×10^5 and 10^6 W/m²K, and the temperature of the center increases in a small slope. The very large air convection coefficient indicates the very small thermal resistance in the numerical scheme. A very

large numerical error is created, and hc of larger than 2×10^5 W/m²K is not considered. hc is between the values of 200 and 2×10^3 W/m²K, the temperature of the center decreases as hc increases. It's because the simulated temperatures of convective boundary condition and the isothermal boundary condition exist a great deviation as the air convection coefficient is decreased. The thermal resistance increases, the differences between the central temperature and the ambient temperature increases. Between the values of 2×10^3 and 2×10^5 W/m²K there exist the lowest value at the temperature profile, an optimal value can be found in this scope. Whereas hc is 2×10^4 W/m²K, the simulated temperature of the center is 331.457K. The temperature of the center is 331.448K with the isothermal boundary condition of 320K. Therefore the isothermal boundary condition replaced by convective boundary condition of infinite heat transfer coefficient in the numerical simulation, a large value of hc is chosen as the value of 2×10^4 W/m²K in the following calculation.

(a)

(b)
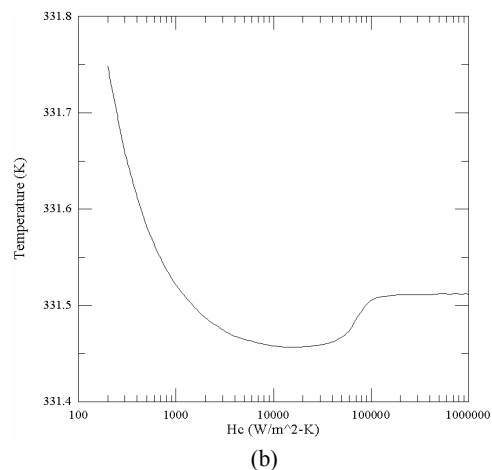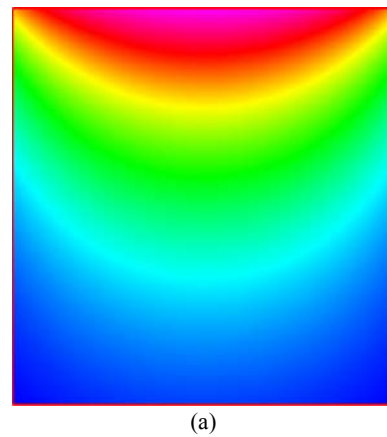
Fig. 9 (a) 2-D square model (b) the temperature profile of the chamber center under various heat convective coefficient

The h_c value of 2×10^4 W/m²K and CFD-ACE+^{TM} user subroutine are utilized to simulate the temperature variations and the temperature distributions of the chamber whereas the chamber passes by each isothermal zone in the system. The convection boundary condition with the h_c value of 2×10^4

World Academy of Science, Engineering and Technology
International Journal of Materials and Metallurgical Engineering
Vol:3, No:5, 2009

W/m^{2}K is utilized to replace the isothermal boundary conditions of 368K, 318K, and 345K. The simulated ambient temperatures are 368K, 318K and 345K, respectively, as the chamber moves in the isothermal zones. Between two isothermal zones the h_c is 10 W/m^{2}K, and the ambient temperature is 300K. The moving speed of the chamber varies from 0.0001 m/s to 1 m/s. Simulation results of the temperature of the chamber center are shown in Fig. 10. As the result shows that the center temperature is not able to achieve 368K at the time of 30 s. The larger moving speed is; the more difference between the chamber temperature and the temperature of the heating block is. However the differences are all within 0.5K. While moving between the isothermal regions, the temperature of the chamber decreases with the air convection. The chamber temperature does not drop to 300K, but it reaches the reaction temperature at the next isothermal region. The result also shows the temperature of the chamber center achieves 318K at 120s. Similarly, the center temperature decreases by the air convective effect between the times of 150 s and 180 s. And then the temperature of the chamber can achieve 345K after moving through the third isothermal region. It's useful to reduce the chamber temperature by air convection between two isothermal zones. The time duration of the chamber moving between two isothermal regions is 30s in this case. The total reaction time per cycle can be reduced if the time duration is decreased. The effects of the various time durations on the chamber temperature are investigated in the future. At 150s, the temperature standard deviations of the chamber are less than 1.4×10^{-3}K with the moving speed between 0.0001 m/s and 1 m/s. The result is not shown.
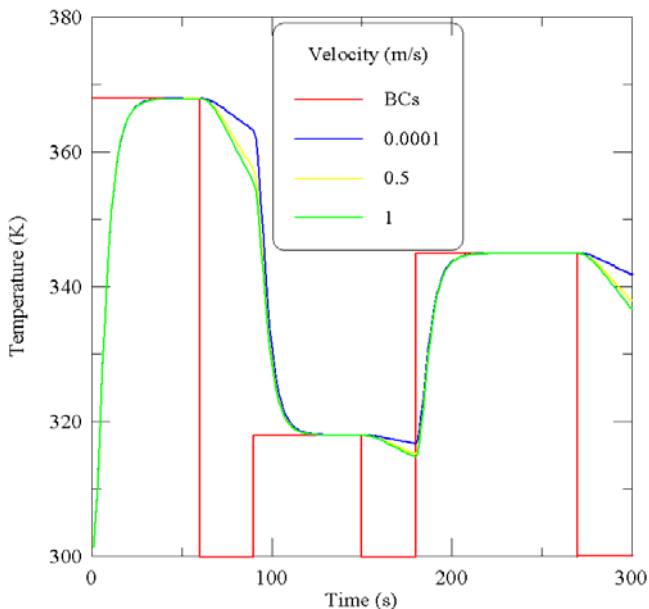

Fig. 10 the center temperature profiles of chamber at various moving speed

The temperature distributions of Y-half cut cross section at three different times of 60 s, 150 s, and 270 s are shown in Fig. 11, respectively. In Fig. 11, the heating faces reducing to four and the air convection boundary conditions used between two isothermal zones there does not exit the higher temperature at back side of chamber as the moving speed is over 0.001 m/s. The uniformity of the temperature distribute inside the chamber can be obtained.
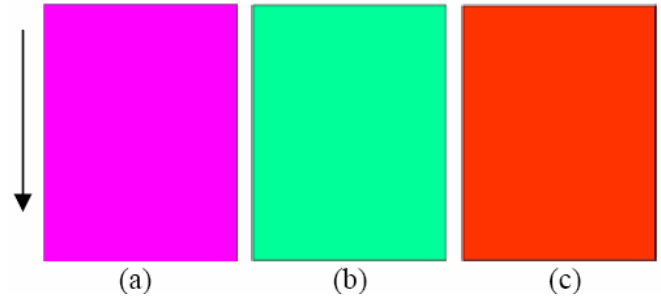

Fig. 11 At the moving speed of 1 m/s, the temperature distribution of Y-half cut cross section at (a) 60 s, (b) 150 s, (c) 270 s

V. CONCLUSION

In order to reduce the reaction time and make temperature distribution uniform in the reaction chamber, a novel oscillatory thermal cycler is designed. The sample is placed in a fixed chamber, and three constant isothermal zones are established in the system. The sample is oscillated and contacted with three different isothermal zones to complete thermal cycles. The influences of various materials on the heat transfer are examined, and the simulation result shows that copper is the best choice. However considering the price and the weight, aluminum is the most proper choice. Regarding to the six heating faces, results show that the moving speed affects the uniformity of the temperature distribution of the chamber. As moving speed is larger than 0.01 m/s, the non-uniform effect of the temperature distribution at the back side of the chamber is very obvious. In order to improve the temperature uniformity, the heating faces are reduced to four, and the convective boundary conditions are set at the front and the back side of the chamber. It's illustrated that by reducing the number of the heating faces the uniformity of the temperature can be improved even the moving speed is larger than 0.01 m/s. The hc value of 2×10^4 W/m^{2}K and CFD-ACE^{+TM} user subroutine are used to simulate the temperature variations and the temperature distributions of the chamber whereas the chamber passes by each isothermal zone in the system. The boundary conditions of the front and the back side of the chamber are set to be heat convection. The conditions of the other four sides are set to be isothermal as the chamber moves through the heating blocks and set to be convective as the chamber moves between two isothermal regions. It's found that the boundary conditions are more realistic than the former two cases and the standard deviations of the temperature distributions are less than 1.4×10^{-3}K. Then the moving speed has little influences on the temperature distribution of the chamber at the assigned time duration. The effects of the various time durations on the chamber temperature are investigated in the future, and then the optimal geometric parameters can be obtained.

World Academy of Science, Engineering and Technology
International Journal of Materials and Metallurgical Engineering
Vol:3, No:5, 2009

REFERENCES

[1] K. Mullis, F. Ferre, R. A. (Eds.), Gibbs, *The Polymerase Chain Reaction*, *Springer*, 1994.

[2] S. H. Kim, J. Noh, M. K. Jeon, K. W. Kim, L. P. Lee, and S. I. Woo, "Micro-Raman Thermometry for Measuring the Temperature Distribution inside the Microchannel of a Polymerase Chain Reaction Chip," *Micromechanics and Microengineering,* Vol. 16, pp. 526–530, 2006.

[3] M. A. Northrup, M. T. Ching, R. M. White, and R. T. Wltson, "DNA Amplification in a Microfabricated Reaction Chamber," *7th International Conference of Solid-State Sensors and Actuators, Transducers '93*, pp. 924-926, 1993.

[4] M. U. Kopp, A. J. D., Mello, and A. Manz, "Chemical Amplification: Continuous-Flow PCR on a Chip," *Science,* Vol. 280, pp. 1046-1048, 1998.

[5] Q. Zhang, W. Wang, H. Zhang, and Y. Wang, "Temperature Analysis of Continuous-Flow Micro-PCR Based on FEA," *Sensors and Actuators B,* Vol. 82, pp.75-81, 2002.

[6] C. F. Chou, R. Changrani, P. Roberts, D. Sadler, J. Burdon, F. Zenhausern, S. Lin, A. Mulholland, N. Swami, and R. Terbrueggen, "A Miniaturized Cyclic PCR Device–Modeling and Experiments," *Microelectronic Engineering,* Vol. 61-62, pp. 921-925, 2002.

[7] M. Bu, T. Melvin, G. Ensell, J. S. Wilkinson, and A. G. R. Evans, "Design and Theoretical Evaluation of a Novel Microfluidic Device to Be Used for PCR," *Journal of Micromecanics Microengineering,* Vol. 13, pp. S125-S130, 2003.

[8] M. Hashimoto, P. C. Chen, M. W. Mitchell, D. E. Nikitopoulos, S. A. Soper, and M. C. Murphy, "Rapid PCR in a Continuous Flow Device," *Lab on a Chip,* Vol. 4, pp. 638-645, 2004.

[9] S. R. Joung, C. J. Kang, and Y. S. Kim, "Series DNA Amplification Using the Continuous-Flow Polymerase Chain Reaction Chip," *Japanese Journal of Applied Physic,* Vol. 47, pp. 1342-1345, 2008.

[10] J. Xiaoyu, N. Zhiqiang, C. Wenyuan, and Z. Weiping, "Polydimethylsiloxane (PDMS)-Based Spiral Channel PCR Chip," in *Proc. 4th Electronics Letters Conf.* Vol. 41, No. 16, 2005.

[11] N. C. Tsai, and C. Y. Sue, "Thermal Control of Micro Reverse Transcription-Polymerase Chain Reaction Systems," S*ensors and Actuators A,* Vol. 136, pp. 178-183, 2007.

[12] T. Nakayama, Y. Kurosawa, S. Furui, K. Kerman, M. Kobayashi, S. R. Raao, Y. Yonezawa, K. Nakano, A. Hino, S. Yamamura, Y. Takamura, and E. Tamiya, "Circumventing Air Bubbles in Microfluidic Systems and Quantitative Continuous-Flow PCR Applications," *Analytical and Bioanalytical Chemistry,* Vol. 386, pp. 1327-1333, 2006.

[13] C. Gartner, R. Klemm, and H. Becker, "Methods and Instruments for Continuous-Flow PCR on a Chip," *Proc. of SPIE,* Vol. 6465, pp. 646502-1-646502-8, 2007.

[14] N. Crews, C. Wittwer, and B. Gale, "Continuous-Flow Thermal Gradient PCR," *Biomed Microdevices,* Vol. 10, pp. 187–195, 2008.

[15] D. S. Lee, and C. S. Chen, "Development of a Temperature Sensor Array Chip and a Chip-Based Real-Time PCR Machine for DNA Amplification Efficiency-Based Quantification," *Biosensors and Bioelectronics,* Vol. 23, pp. 971-979, 2008.

Jyh-Jian Chen received the BS degree, the MS degree and the PhD degree in mechanical engineering from National Chiao Tung University, Taiwan, ROC, in 1991, 1992 and 1999, respectively. In 1999–2004, he worked as an associate researcher at Precision Instrument Development Center, Taiwan, ROC, where he focuses on the development of optomechanical systems for remote sensing applications. In 2004-2006, he has been Industrial Technology Research Institute, Taiwan, ROC, as an engineer in the Bio Microfluidic Technology Department. Since autumn 2006, he worked as an assistant professor at Department of Biomechatronics Engineering, National Pingtung University of Science and Technology, Taiwan, ROC. His research interests are Microfluidics, and BioMEMS as well as Computational Simulation.

Tse-Yu Hsieh received the BS degree in Biomechatronics Engineering from National Pingtung University of Science and Technology, Taiwan, ROC, in 2007. In 2007–2009, he studied as a master at National Pingtung University of Science and Technology, Taiwan, ROC, where he focuses on the development of PCR systems for temperature sensing, and heater applications. His research interests are Heat Transfer, and System Assembly as well as Computational Simulation.

Open Science Index, Materials and Metallurgical Engineering Vol:3, No:5, 2009 publications.waset.org/10480.pdf